Int J Fract (2013) 179:229–235
DOI 10.1007/s10704-012-9780-5
© Springer Science+Business Media Dordrecht 2012

LETTERS IN FRACTURE AND MICROMECHANICS

EVALUATION OF THE GROWTH OF DISLOCATIONS DENSITY IN FATIGUE LOADING PROCESS VIA ELECTRICAL RESISTIVITY MEASUREMENTS.

Mohammad A. Omari and Igor Sevostianov[1]

Department of Mechanical and Aerospace Engineering, New Mexico State University. Las Cruces, NM 88003, USA.

[1] Author for correspondence, igor@nmsu.edu

Abstract. The paper focuses on quantitative evaluation of the microstructural changes - growth of the dislocation density - in stainless steel specimens subjected to fatigue loading. We propose to use electrical resistivity measurements for this goal. Change in electrical resistance of the specimens has been monitored in dependence on the number of fatigue cycles and the relative growth of the dislocation density was calculated from these data and known values of the specific resistivity of dislocations for iron. We also estimated the growth of dislocation density using analysis of Scanning Electron Microscopy (SEM) images of etched specimens. This estimate however appears to be unreasonably low, so that SEM may be used for qualitative analysis only.

Keywords: dislocation density, electrical resistivity, fatigue.

1. Introduction

Several methods have been developed to estimate dislocation density (number of dislocations crossing a unit area or the sum of dislocation length per unit volume) in metals and alloys. These methods can be subdivided on to five main groups (Hull and Bacon, 2011): (1) surface method, (2) decoration method, (3) electron microscopy, (4) X-ray diffraction, and (5) field emission and field ion microscopy. Probably, the most common method is combination of the etch pit technique with microscopy (Malta *et al*, 1992; Yonenaga *et al*, 2001). Note that all of the standard methods of experimental measurement of the dislocation density are both expansive and time-consuming, so that the problem of the *in situ* evaluation of this quantity in the context of various engineering applications is still open. We propose to use elect5rical conductivity measurements for this goal.

Starting from 1930s, many techniques have been proposed to estimate dislocation density ρ in metals. Gay *et al* (1953) suggested using X-ray images for this aim. They obtained the following dependence of the dislocation density on the angle α between two grains, length of the Burgers vector *b*, and the block size *t*: $\rho = \frac{\alpha}{bt}$. More recently, Hoque *et al* (2005) applied pattern recognition and image processing techniques to quantitatively measure the changes in microstructure of metals under different type of treatment in order to increase tool life. Shintani and Murata (2011) applied X-ray diffraction, Transmission Electron Microscopy (TEM) and Vickers hardness tests to quantitatively evaluate the change in dislocations density and dislocations character in stainless steel 304. They showed that two factors have strongest effect on changes in mechanical properties: formation of strain-induced second phase and work-hardening induced by increase in dislocation densities. The average dislocations density was observed to be around $5x10^{14}$ m^{-2}. Chen and Duggan (2004) utilized TEM microscopy to measured dislocation density for Interstitial-Free steel during cold rolling at low reduction, their results showed the dislocation density was up to $3x10^{14}$ m^{-2}.

Field et al. (2012) used automated electron backscatter diffraction scanning to study dislocations density for deformed Cu, Al and steel specimens. The results were depending on the dislocation cell size. They determined dislocation density for step size 0.1 μm which was $2x10^{15}$

m^{-2}. Ahmed *et al* (2006) and Gutierrez-Urrutia and Raabe (2012) studied SEM with electron channeling contrast imaging (ECCI) technique to reveal dislocation structures for the bulk samples. The advantages of this method are as follows: low requirements for specimen preparation (no precise polishing is required for example), the method is sufficiently simple and accurate. The dislocation density is calculated as $\rho = \frac{2N}{Lt}$ where N is the number of dislocation lines intersecting a grid of total line L and t is the specimen thickness. They also compared their results with ones obtained by analysis of transmission electron microscope (TEM) images. Eisenlohr *et al* (2008) suggested a new method to quantify the local dislocation spacing on sections displaying the intersections of dislocation lines. They applied this method to evaluate dislocation density in single crystal of CaF_2.

Connection between dislocation density growth and formation of microcracks has been studied by Alvarez-Armas *et al* (2012) who evaluated the damage in fatigued stainless steel. Their analysis of the dislocation structure in the near-surface and in ferritic grains shows that dislocation microbands are associated with microcracks initiation.

The present work is motivated by results of Yulianto *et al* (2012) who applied this technique in the process of quasi-static loading for titanium. In the present paper, the dislocation density is evaluated using electrical resistance measurements and analysis of scanning electron microscope (SEM) images for fatigued SS304 specimens. The resistance of specimens and SEM images were measured before and after fatigue process. The increase in dislocation density was evaluated from resistivity measurements and from analysis of SEM images.

2. Experimental methods

Stainless Steel 304 sheet has thickness of 1.905 mm has been purchased from TA CHEN INTERNATIONAL. The reported chemical composition of the material is as follows: C 0.08 max, Cr 18 – 20%, Fe 66.5 – 74%, Mn 2% max, Ni 8 - 10.5%, P 0.045% max, S 0.03% max, Si 1% max. Mechanical properties reported by the manufacturer are given in Table 1.

Young Modulus	Ultimate Tensile Strength	Yield Strength	Electrical Resistivity
193 GPa	505 MPa	215 MPa	720 $e^{-9}\Omega$.m

Table 1. Mechanical properties of stainless steel 304 reported by the manufacturer.

To cut the specimens a water jet cutter was used. It provides continuous cooling during the cutting process to avoid any changes in mechanical properties. Geometry of the specimens was selected in accordance with the ASTM 557M standard (Figure 1). A small rectangular damage initiation notch was introduced in the center of each specimen.

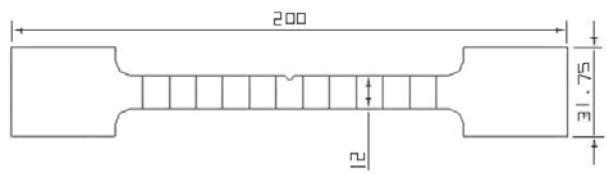

Figure 1. Geometry of the specimen. All the dimensions are in millimeters.

Fatigue tests were performed using MTS Landmark Servo Hydraulic Test System at 20Hz. Specimens were tested under maximum fatigue loading of $c_{max} = 215\,MPa$ with $R = c_{min}/c_{max} = 0.1$ for different number of cycles: 10,000; 20,000; 30,000 and 50,000 cycles. Initial resistances readings were scanned at eleven different locations on each specimen using HP

4338B milliohmmeter by four-probe method with high accuracy; the distance between two probes is 14 mm. After the loading, the resistances were scanned again.

Before and after loading, microstructure of specimens has been tested with Scan Electron Microscope (SEM) model Hitachi S-3400N that has accelerating voltages 0.3 kV to ~30 kV and magnification range 5x to 300,000x. Best images were taken at 6000x magnification using 10 kV accelerating voltage. All the measurements were repeated on ten specimens and the data were averaged.

3. Results and Discussion

To calculate the dislocation density changes before and after fatigue process we used two different methods (1) electrical resistance measurements and (2) image processing of the SEM images.

Connection between changes in dislocation density and electrical resistivity of metals has been widely discussed in literature starting from 1970s. Watts (1988 a, b) has shown how atomic disorder near dislocation line can produce enough large-angle scattering to account for the measured values of electrical resistivity in metals. He stated that to understand the physical origin of the electrical resistivity in a discrete model, one must focus on the crucial point that a discrete model potential must somehow produce much more large-angle scattering from the region near a dislocation line than can be produced by the continuum model. Watts (1988b) considered an example of an electron's wave vector being near a dislocation line with two different situations. One in which it is in an undeformed hypothetical Brillouin zone and another in which it is in a deformed hypothetical Brillouin zone. If the electron were to travel into the deformed region it would be Bragg Deflected. On the other hand if the electron was close to the undeformed Brillouin zone it would only take a small strain to produce Bragg scattering.

Quantitative estimates of the effect of dislocation density on electrical resistivity of various methods have been done in works of Brown (1977) and Karolik and Luhvich (1994). They analytically predicted specific resistivity of dislocations for a number of metals that is close to experimentally obtained. For instance, experimentally measured specific dislocation resistivity (resistivity of dislocations per unit dislocation density N) of iron R^d/N is $10\pm4\times10^{-19}$ Ωcm^3 (Tanaka and Watanabe, 1972); its theoretical estimate by Karolik and Luhvich (1994) is 12.6×10^{-19} Ωcm^3.

For isotropic distribution of dislocations, increase in resistivity of a specimen can be expressed in terms of the dislocation density growth as

$$\Delta R \equiv R - R^0 = \Delta\rho R^d / N \tag{1}$$

Solving this equation for $\Delta\rho$, we get

$$\Delta\rho = \frac{N\left(R - R^0\right)}{R^d} \tag{2}$$

Results of the calculation of the dislocation density changes are given in Table 2.

sample 10 k	sample 20 k	sample 30 k	sample 50 k
6.21E-09	1.22854E-08	1.26381E-08	1.40651E-08
6.20904E-09	1.28556E-08	1.44183E-08	1.46672E-08
4.7605E-09	7.73357E-09	1.46592E-08	1.58774E-08
1.21191E-08	1.27268E-08	1.39513E-08	1.37157E-08
1.52174E-08	1.74159E-08	2.21448E-08	3.00961E-08
1.56156E-08	1.89159E-08	2.29513E-08	2.08339E-08
7.30071E-09	9.45793E-09	1.18858E-08	1.41869E-08
5.46404E-09	1.04336E-08	1.24579E-08	1.09646E-08
4.31249E-09	1.25264E-08	1.388E-08	1.35564E-08
8.0907E-09	1.13748E-08	1.10595E-08	1.13411E-08
8.47564E-09	1.22701E-08	1.29174E-08	1.26106E-08
8.52502E-09	1.25451E-08	1.48149E-08	1.56286E-08
Density calculations : $\Delta\rho = \frac{N(R - R^0)}{R^d}$			
8.52502E+15	1.25451E+16	1.48149E+16	1.56286E+16

Table 2. Results of calculation of the dislocation density from resistivity measurements (averaged over ten specimens)

Figure 2 illustrates the dependence of the dislocations density on the number of cycles in the fatigue process for $c_{max} = 215\,MPa$ (5000 N) calculated using electrical resistivity measurements according to (2).

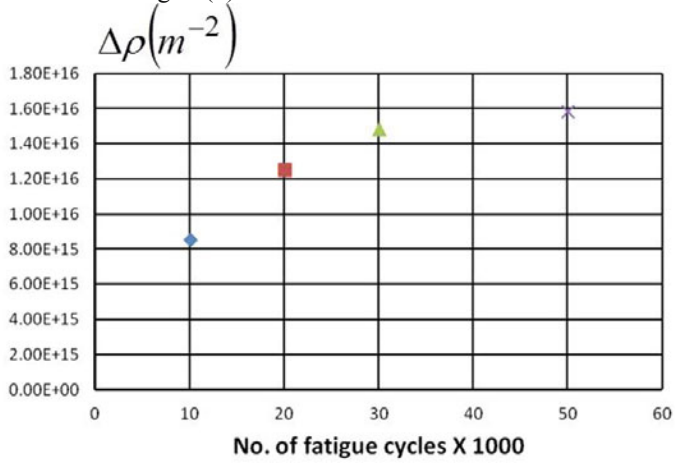

Figure 2. Dislocation density calculated from resistivity measurements as a function of a number of fatigue cycles

Image processing technique was applied to the SEM images to calculate the dislocation density. Figure 3 shows typical microstructures corresponding to different number of cycles of loading. Dislocations are responsible for both black dots ("pits") and white dots ("hillocks") (Hull and Bacon, 2011). Vogel *et al* (1953) experimentally established one–to-one relation between these pits and the dislocation lines.

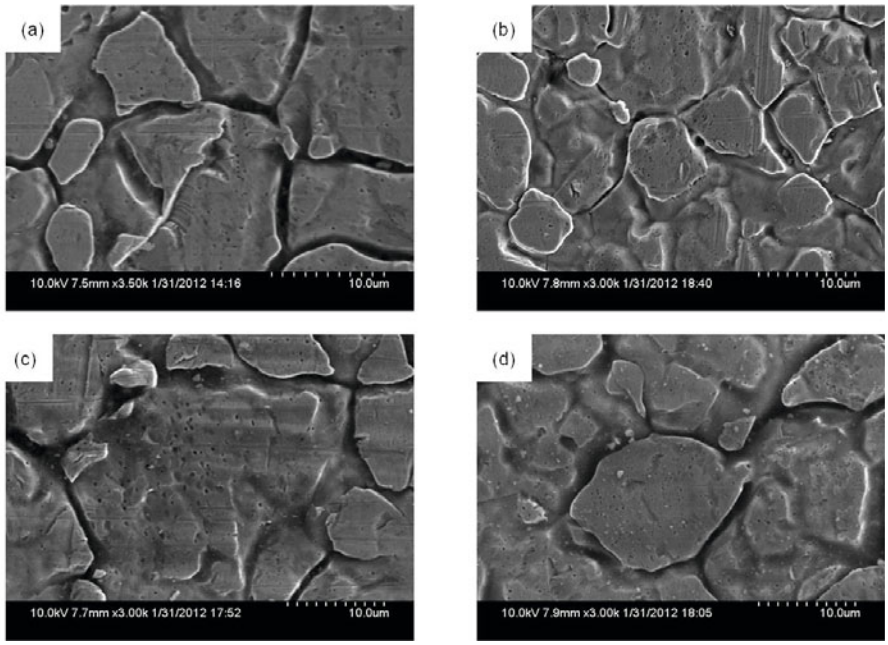

Figure 3. Microstructure of specimens after (a) 10000, (b) 20000, (c) 30000 and (d) 50000 cycles

We used SEM images to calculate the dislocation density as shown in Figure 4 which shows original image, its binary modification where we converted the background to white and the pits to be counted to black, and the counting image.

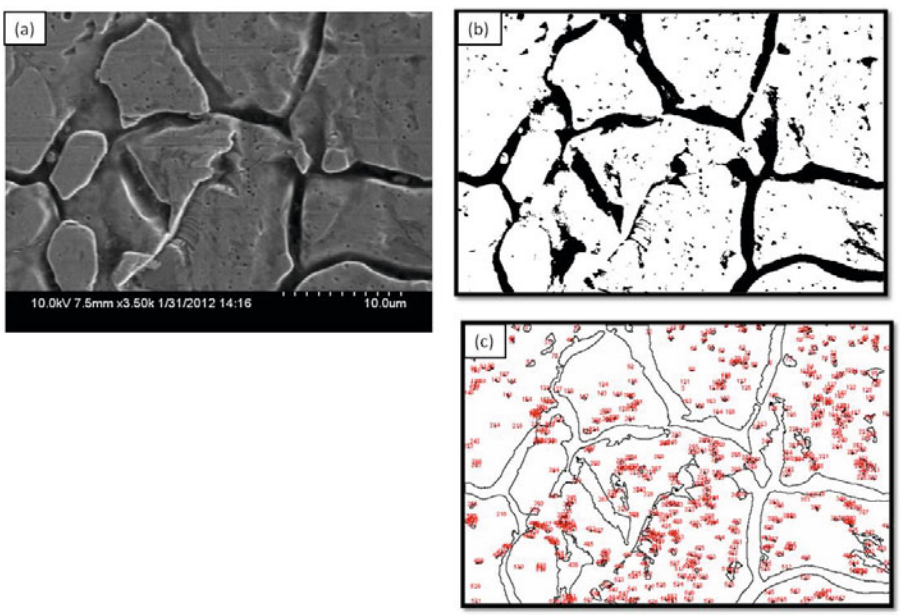

Figure 4. Example of calculation of the dislocation density from SEM images: (a) the original SEM image, (b) image changed to binary one, (c) counting the black dots

The results of images analysis are summarized in Figure 5. It is seen that obtained dislocation densities are unreasonably small. It means that SEM images are insufficient for such analysis – not all the dislocation lines can be seen.

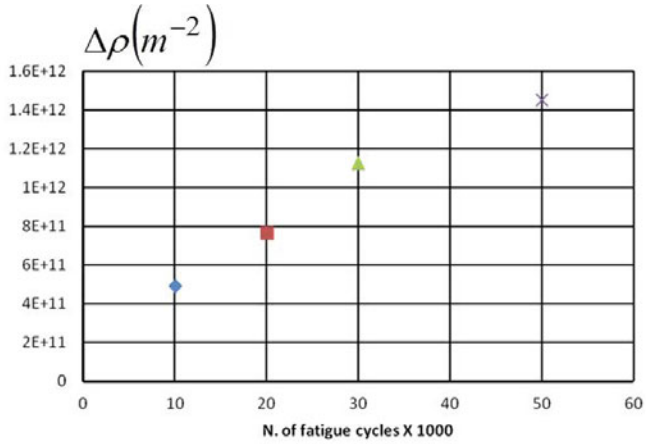

Figure 5. Dislocation density estimated from the analysis of SEM images.

4. Conclusions

In this paper we focused on the evaluation of the density of dislocations produced during cyclic loading of stainless steel 304 specimens. For this goal we used electrical resistivity measurements and analysis of SEM images. Comparison of the results with the published ones (Yulianto et al.,2012 ; Field et al.,2012; Hoque et al.,2005; Chen and Duggan, 2004) allows us to state that estimation of the dislocation density from resistivity measurements produces reasonable results while analysis of SEM images gives dislocation density three orders of magnitude lower than expected. It means that SEM technique itself cannot be used for evaluation of the dislocation density. It has to be supplemented, for example, by ECCI technique (Gutierrez-Urrutia and Raabe, 2012).

Acknowledgement. The financial support of New Mexico Space Grant Consortium is gratefully acknowledged.

References

Ahmed, J., Roberts, S. G. and Wilkinson, A. J. (2006) Characterizing dislocation structure evolution during cyclic deformation using electron channeling contrast imaging. *Philosophical Magazine*, **86**, 4965–4981.

Armas, A., Krupp, U., Balbi, M., Herenu, S., Marinelli, M. and Knobbe, H. (2012) Growth of short cracks during low and high cycle fatigue in a duplex stainless steel. *Int. J. of Fatigue*, **41**, 95–100.

Brown, R. A. (1977) Electrical resistivity of dislocations in metals. *J. Phys. F: Metal Phys*, **7**, 1283-1295.

Chen, Q. Z., and Duggan, B. J. (2004) On Cells and Microbands Formed in an Interstitial-Free Steel during Cold Rolling at Low to Medium Reductions. *Metallurgical and materials transactions A*, **35**, 3423-3430.

Eisenlohr, P., Sadrabadi, P., Blum, W. (2008) Quantifying the distributions of dislocation spacings and cell sizes. *J. Mater Sci*., **43**, 2700–2707.

Field, D. P., Merriman, C., Allain-Bonasso, N., and Wagner, F. (2012) Quantification of dislocation structure heterogeneity in deformed polycrystals by EBSD. *Modelling Simul. Mater. Sci. Eng*. **20**, 1-12.

Gay, P., Hirsch, P. b., and Kelly, A. (1953) The estimation of dislocation densities in metals from X-Ray data. *Acta metallurgica*, **1**, 315-319.

Gutierrez-Urrutia, I., and Raabe, D. (2012) Dislocation density measurement by electron channeling contrast imaging in a scanning electron microscope. *Scripta Materialia*, **66**, 343–346.

Hoque, M. E., Ford, M. R., and Roth, J. T. (2005) Automated Image Analysis of Microstructure Changes in Metal Alloys*. The int. society for optical engineering*, **5679**, 1-9.

Hull, D. and Bacon, D. J. (2011) *Introduction to Dislocations,* Butterworth-Heinemann, London.

Karolik, A. S. and Luhvich, A. A. (1994) Calculation of electrical resistivity produced by dislocations and grain boundaries in metals. *J. Phys: Condens. Matter* **6**, 873-886.

Malta, D. P., Posthill, J. B., Markunas, R. J. and Humphreys, T. P. (1992) Low-defect- density germanium on silicon obtained by a novel growth phenomenon. *Appl. Phys.Letters,* **60**, 844-846.

Shintani, T. and Murata, Y. (2011) Evaluation of the dislocation density and dislocation character in cold rolled Type 304 steel determined by profile analysis of X- ray diffraction. *Acta Materialia*, **59**, 4314–4322.

Vogel, F. L., Pfann, W. G., Corey, H. E. and Thomas, E. E. (1953) Observations of Dislocations in Lineage Boundaries in Gerinanium. *The American Physical Society*, **90**, 489-490.

Watts, B.R. (1988a) The contribution of the long-range strain field of dislocations in metals to their electrical resistivity, *J. Phys. F: Met. Phys.,* **18**, 1183-1195

Watts, B.R. (1988b) Calculation of electrical resistivity produced by dislocations in various metals, *J. Phys. F: Met. Phys.,* **18**, 1197-1209.

Yonenaga, I., Taishi, T., Huang, X. and Hoshikawa, K. (2001) Dynamic characteristics of dislocations in highly boron-doped silicon. *J. Appl. Phys*, **89**, 5788-5790.

Yulianto, I. Omari, M. and Sevostianov, I. (2012) Evaluation of changes in dislocation density in TI-CP2 in the process of quasi-static loading using electrical resistance measurement. *Int. J. Fracture*, **175**, 73-78.

Tanaka, K. and Watanabe, T. (1972) An electrical resistivity study of lattice defects, *Applied Physics*, **11**, 1429-1439.